

**Thermodynamic quantities of metals investigated by an analytic statistical moment method**K. Masuda-Jindo,<sup>1</sup> Vu Van Hung,<sup>2</sup> and Pham Dinh Tam<sup>2</sup><sup>1</sup>*Department of Materials Science and Engineering, Tokyo Institute of Technology, Nagatsuta 4259, Midori-ku, Yokohama 226-8503, Japan*<sup>2</sup>*Department of Physics, Hanoi National Pedagogic University, km8 Hanoi-Sontay Highway, Hanoi, Vietnam*

(Received 18 June 2002; published 5 March 2003)

The thermodynamic properties of metals are studied by including explicitly the anharmonic effects of the lattice vibrations going beyond the quasiharmonic approximations. The free energy, thermal lattice expansion coefficients, mean-square atomic displacements, and specific heats at the constant volume and those at the constant pressure,  $C_v$  and  $C_p$ , are derived in closed analytic forms in terms of the power moments of the atomic displacements. The analytical formulas give highly accurate values of the thermodynamic quantities, which are comparable to those of the molecular dynamics or Monte Carlo simulations for a wide temperature range. The present formalism is well suited to calculate the thermodynamic quantities of metals and alloys by including the many body electronic effects and by combining it with the first-principles approaches.

DOI: 10.1103/PhysRevB.67.094301

PACS number(s): 64.10.+h, 65.40.-b

**I. INTRODUCTION**

The first-principles determination of the thermodynamic quantities of metals and alloys are now of great importance for the understanding of structural phase transformations as well as for the phase diagrams computations.<sup>1-3</sup> So far, the first-principles density functional theories<sup>4-8</sup> have been used extensively for the calculations of the ground state properties of various metal systems at the absolute zero temperature. In the phase transformations occurring in metals and alloys at finite temperatures (under pressure  $P$ ), the thermal lattice vibrations (anharmonicity effects) play an essentially important role.<sup>9,10</sup> However, most of the first-principles calculations for the structural phase transformations and alloy phase diagram computations have been done with the use of the lattice vibration theory in the quasiharmonic (QH) approximation.<sup>11-15</sup> For the alloy phase diagram calculations, there have been difficulties in accounting for the anharmonicity of thermal lattice vibrations, especially for the higher temperature region than the Debye temperature because the thermal lattice expansion plays an important role and cannot be neglected. The martensitic phase transformation in substitutional alloys such as the  $\text{Ni}_x\text{Al}_{1-x}$  system has also been studied with the QH approximation, and the temperature region treated by the QH theory is usually lower than the Debye temperature.<sup>16</sup>

The systems considered at high temperatures and high pressures require the allowance for anharmonic effects which are very essential in these regions. The simplest way is to use the QH Debye-Grüneisen theory.<sup>10</sup> However, the results obtained in such a way are not always satisfactory. It is noted that the Debye form of the harmonic approximation is rather crude theory. The applicability of the QH method to the study of particular metals is often restricted by the isotropic Debye mode and the assumption of the mean sound velocity  $v$ .<sup>17</sup> The temperature dependence of the lattice constant and the linear thermal expansion coefficient are calculated by minimizing the free energy with respect to the volume of the system. Due to their simplicity, pair potentials are often used

for genetic studies of trends among a given class of metallic materials. Therefore, they do not account for mostly important many-body electronic effects in metallic systems, and they cannot be relied on for properties of real materials.

A number of theoretical approaches have been proposed to overcome the limitations of the QH theories. The first calculation of the lowest-order anharmonic contributions to the atomic mean-square displacement  $\langle u^2 \rangle$  or the Debye-Waller factor was done by Maradudin and Flinn<sup>18</sup> in the leading-term approximation for a nearest-neighbor central-force model. Since then, many anharmonic calculations including the lowest-order anharmonic contributions have been performed for metal systems.<sup>19,20</sup> The method requires acknowledgement of a number of Brillouin-zone sums<sup>14</sup> and the calculations are performed for the central-force model crystals. Recently, some attempts have been made to take into account the bond length dependence of bond stiffness tensors in the calculations of the free energy of the substitutional alloys.<sup>21,22</sup> The anharmonic effects of lattice vibrations on the thermodynamic properties of the materials have also been studied by employing the first-order quantum-statistical perturbation theory<sup>23-25</sup> as well as by the first-order self-consistent (SC) phonon theories.<sup>26-31</sup> The theories have been used to analyze, e.g., the temperature dependence of extended x-ray absorption fine-structure (EXAFS) spectra and the phonon frequencies. However, the previous anharmonicity theories are still incomplete and have some inherent drawbacks and limitations.

In the present study, we use the finite-temperature moment expansion technique to derive the Helmholtz free energies of metal systems, going beyond the QH approximations. The thermodynamic quantities, mean-square atomic displacements, specific heats, and elastic moduli are determined from the explicit expressions of the Helmholtz free energies. The Helmholtz free energy of the system at a given temperature  $T$  will be determined self-consistently with the equilibrium thermal lattice expansions of the crystal.

We will use the electronic many-body potentials, i.e., second-moment tight-binding (TB) potentials,<sup>32-40</sup> for the

evaluation of the internal energy of the system. In metals the long-range Coulomb interaction and the partially filled valence bands lead to interatomic forces that are inherently many-body in nature. For more than a decade, the embedded-atom method (EAM)<sup>41–45</sup> and the second-moment approximation (SMA) of the TB scheme have been the two most common approaches, able to overcome the major limitations of two-body pair potentials.<sup>18,46,47</sup> The physical basis of EAM models makes them valid, especially for normal or noble metals, whereas SMA is *a priori* well suited for transition elements (with narrow *d*-band bonding).

In Sec. II, we will make a general derivation of the thermal lattice expansion and Helmholtz free energy of the monoatomic cubic metals based on the fundamental principles of quantum-statistical mechanics. The thermodynamic quantities of the metals are then derived in terms of the power moments of the atomic displacements from the Helmholtz free energy of the system. Section III includes our main calculation results of the thermodynamic quantities of some cubic metals. Finally, Sec. IV summarizes the present study.

## II. THEORY

We derive the thermodynamic quantities of metals, taking into account the higher- (fourth-) order anharmonic contributions in the thermal lattice vibrations going beyond the QH approximation. The basic equations for obtaining thermodynamic quantities of the given crystals are derived in a following manner: The equilibrium thermal lattice expansions are calculated by the force balance criterion and then the thermodynamic quantities are determined for the equilibrium lattice spacings. The anharmonic contributions of the thermodynamic quantities are given explicitly in terms of the power moments of the thermal atomic displacements.

Let us first define the lattice displacements. We denote  $\mathbf{u}_{il}$  the vector defining the displacement of the *i*th atom, in the *l*th unit cell, from its equilibrium position. The potential energy of the whole crystal  $U(\mathbf{u}_i)$  is expressed in terms of the positions of all the atoms from the sites of the equilibrium lattice. We may assume that this function has a minimum when all the  $\mathbf{u}_{il}$  are zero, for the perfect lattice is presumably a configuration of stable equilibrium. We use the theory of small atomic vibrations, and expand the potential energy  $U$  as a power series in the Cartesian components,  $u_{il}^j$ , of the displacement vector  $\mathbf{u}_{il}$  around this point

$$U = U_0 + \sum_{i,l,j} \left[ \frac{\partial U}{\partial u_{il}^j} \right]_{\text{eq}} u_{il}^j + \sum_{ii',ll',jj'} \left[ \frac{\partial^2 U}{\partial u_{il}^j \partial u_{i'l'}^{j'}} \right]_{\text{eq}} u_{il}^j u_{i'l'}^{j'} + \dots, \quad (1)$$

where  $U_0$  denotes the internal (cohesive) energy of the system. If we truncate the above expansion of Eq. (1) up to the second-order terms, then the full interatomic potential is replaced by its quadratic expansion about the equilibrium atomic positions. The system is then equivalent to a collection of harmonic oscillators, and diagonalization of the corresponding dynamical matrix yields the squares of the

normal-mode frequencies (phonon spectrum).<sup>48</sup> This scheme is called as the QH approximation.

In the present study the thermodynamic quantities are calculated with the use of the electronic many-body potentials or the potentials derived by EAM. We note that the present analytic formulation is quite useful when we combine it with the *ab initio* theoretical scheme by numerically evaluating the harmonic  $k$  and anharmonic  $\gamma_1$  and  $\gamma_2$  parameters which will be defined in the subsequent derivations. The SMA TB scheme is well suited to describe the cohesion of transition metals since they are elements with a partially filled narrow *d* band superimposed on a broad free-electron-like *s-p* band. The narrowness of the *d* band, especially in the 3*d* series, is a consequence of the relative constriction of the *d* orbitals compared with the outer *s* and *p* orbitals. As one moves across the periodic table, the *d* band is gradually being filled. Most of the properties of the transition metals are characterized by the filling of the *d* band and ignoring the *sp* electrons. This constitutes Friedel's *d*-band model which further assumes a rectangular approximation for the density of states  $\rho_i(E)$  such that the bonding energy of the solid is primarily due to the filling of the *d* band and proportional to its width. In the SMA, the bonding energy is then proportional to the root of the second moments  $\sqrt{\mu_i^{(2)}}$ . In metals, an important contribution to the structure comes from the repulsive term represented as a sum of pair potentials accounting for the short-range behavior of the interaction between ions. Therefore, the cohesive energy of a transition metal consists of

$$E_{\text{coh}} = E_{\text{rep}} + E_{\text{bond}}. \quad (2)$$

The SMA has been used to suggest various functional form for interatomic potentials in transition metals such as the Finnis-Sinclair potential,<sup>34</sup> the closely related embedded atom potential, and the TB SMA, also referred in the literature as to Gupta potential.<sup>33</sup> The functional form we adopted here for elemental metals is that of the many-body SMA potential

$$E_{ci} = \frac{1}{N} \sum_{i=1}^N \left( A \sum_{j \neq i}^N \exp \left[ -p \left( \frac{r_{ij}}{r_0} - 1 \right) \right] - \left\{ \xi_{ij}^2 \sum_{j \neq i}^N \exp \left[ -2q \left( \frac{r_{ij}}{r_0} - 1 \right) \right] \right\}^{1/2} \right), \quad (3)$$

which has five parameters:  $\varepsilon_0$ ,  $\xi_{ij}$  (for pure metals,  $\xi_{ij} = \xi_0$ ),  $p$ ,  $q$ , and  $r_0$ . The total cohesive energy  $E_c$  of the system is then written as the sum of the  $E_{ci}$ . The parameters  $A$ ,  $\xi_0$ ,  $p$ , and  $q$  are fitted to reproduce some experimental quantities *at zero temperature* (cohesive energy  $E_c$ , lattice parameter  $a$ , bulk modulus and elastic constants). In the summations over the index  $j$  in Eq. (3) are either limited to the  $Z_1$  first neighbors only, and in that case we use the parameters  $A$ ,  $\xi_0$ ,  $p$ , and  $q$  determined by Rosato, Guillope, and Legrand,<sup>35</sup> or extended up to the fifth neighbors, and in that case we use the parameters of Cleri and Rosato.<sup>36</sup> Cleri and Rosato<sup>36</sup> fitted these parameters to experimental data for 16 fcc and hexagonal-close-packed (hcp) transition metals.

TABLE I. Parameters of the second moment TB potentials for cubic metals.

	A (eV)	$\xi$ (eV)	$p$	$q$	$E_c$ (eV/atom)	$a$ (Å)
Al(1) <sup>a</sup>	0.1221	1.316	8.612	2.516	-3.339	4.050
Al(2) <sup>b</sup>	0.0334	0.7981	14.6147	1.112	-3.339	4.050
Ni	0.1368	1.7558	10.00	2.70	-4.435	3.523
Cu	0.0993	1.3543	10.08	2.56	-3.544	3.615
Rh	0.0629	1.660	18.450	1.867	-5.752	3.803
Pd	0.1746	1.718	10.867	3.742	-3.936	3.887
Ag(1) <sup>a</sup>	0.1028	1.1780	10.928	3.139	-2.960	4.085
Ag(2) <sup>b</sup>	0.1231	1.2811	10.12	3.37	-2.960	4.085
Au	0.2061	1.790	10.229	4.036	-3.779	4.079
Pt	0.2975	2.695	10.612	4.004	-5.853	3.924
Li	0.0333	0.3249	7.75	0.737	-1.63	3.49
Na	0.0159	0.2910	10.13	1.30	-1.13	4.29
K	0.0205	0.2625	10.58	1.34	-0.93	5.24
Rb	0.0194	0.2464	10.48	1.40	-0.85	5.61
Cs	0.0205	0.2421	9.62	1.45	-0.80	6.04

<sup>a</sup>indicates parameters taken from Ref. 36.

<sup>b</sup>indicates parameters taken from other sources: Al(2) from Ref. 60 and Ag(2) from Ref. 35.

The SMA TB potentials have been further extended and revised not only for bulk metal systems but also for nanoscale materials. For Rh clusters, Chein, Blaston-Barojas, and Pederson<sup>38</sup> proposed the size-dependent parameters of the SMA TB potentials, on the basis of their generalized gradient approximation (GGA) calculations. A different parametrization strategy was introduced by Sigalas and Papaconstantopoulos<sup>39</sup> in which the parameters were fitted to local density approximation (LDA) calculations of the total energy as a function of lattice constant. Li, Barojas, and Papaconstantopoulos<sup>40</sup> fitted the SMA TB potential parameters to a LDA database that consists of the total energy as a function of the lattice constant for both bcc and fcc lattices, rather than the fitting procedure to experimental quantities. To simulate the long-range nature of the metallic bonding by *sp* electrons in alkali metals, the interactions up to 12th-neighbor shells (228 atoms in bcc crystal) are taken into account.<sup>40</sup> Their potentials fitted to the first-principles LDA results are available for various metals, and more refined nonorthogonal basis TB schemes<sup>39</sup> are also proposed for the quantitative calculations. The present thermodynamic formulation is well suited to couple with any kind of TB schemes mentioned above. The SMA TB potential parameters used in the present calculations are given in Table I.

We now consider a quantum system, which is influenced by supplemental forces  $\alpha_i$  in the space of the generalized coordinates  $q_i$ .<sup>49-51</sup> For simplicity, we only discuss monoatomic metallic systems, and hereafter omit the indices  $l$  on the sublattices. Then, the Hamiltonian of the crystalline system is given by

$$\hat{H} = \hat{H}_0 - \sum_i \alpha_i \hat{q}_i, \quad (4)$$

where  $\hat{H}_0$  denotes the crystalline Hamiltonian without the supplementary forces  $\alpha_i$  and the carets represent operators.

The supplementary forces  $\alpha_i$  act in the direction of the generalized coordinates  $q_i$ . The thermodynamic quantities of the harmonic crystal (harmonic Hamiltonian) will be treated in the Einstein approximation. In this respect, the present formulation is similar conceptually to the treatment of quantum Monte Carlo method by Frenkel.<sup>52,53</sup>

After the action of the supplementary forces  $\alpha_i$  the system passes into a new equilibrium state. For obtaining the statistical average of an thermodynamic quantity  $\langle q_k \rangle_a$  for the new equilibrium state, we use the general formula for the correlation. Specifically, we use a recurrence formula<sup>54</sup> based on the density matrix in the quantum statistical mechanics (for more details see Appendix A)

$$\langle \hat{K}_{n+1} \rangle_a = \langle \hat{K}_n \rangle_a \langle \hat{q}_{n+1} \rangle_a + \theta \frac{\partial \langle \hat{K}_n \rangle_a}{\partial \alpha_{n+1}} - \theta \sum_{m=0}^{\infty} \frac{B_{2m}}{(2m)!} \left( \frac{i\hbar}{\theta} \right)^{2m} \left\langle \frac{\partial \hat{K}_n^{(2m)}}{\partial \alpha_{n+1}} \right\rangle_a, \quad (5)$$

where  $\theta = k_B T$ ,  $m$  is the atomic mass, and  $\hat{K}_n$  is the correlation operator of the  $n$ th order:

$$\hat{K}_n = \frac{1}{2^{n-1}} [\dots [\hat{q}_1, \hat{q}_2]_+ \hat{q}_3]_+ \dots]_+ \hat{q}_n]_+. \quad (6)$$

In Eq. (5) above, the symbol  $\langle \dots \rangle$  expresses the thermal averaging over the equilibrium ensemble with the Hamiltonian  $\hat{H}$  and  $B_{2n}$  denotes the Bernoulli numbers.  $[q_i, q_j]_+$  represents the anticommutation relation. The general decoupling formula of Eq. (5) enables us to get all moments of the lattice system and to investigate the nonlinear thermodynamic properties of the materials, taking into account the anharmonicity of the thermal lattice vibrations. The Helmholtz free energy

of the system can then be obtained by taking into account the higher-order moments (up to fourth order).

The atomic force acting on a given  $i$ th atom in the lattice can be evaluated by taking derivatives of the internal energy of the  $i$ th atomic site and evaluating the power moments of the atomic displacements. If the  $i$ th atom in the lattice is affected by a supplementary force  $\alpha_\beta$ , then the total force acting on it must be zero, and one gets the force balance relation as

$$\sum_{\alpha} \left( \frac{\partial^2 E_{ci}}{\partial u_{i\alpha} \partial u_{i\beta}} \right)_{\text{eq}} \langle u_{i\alpha} \rangle + \frac{1}{2} \sum_{\alpha, \gamma} \left( \frac{\partial^3 E_{ci}}{\partial u_{i\alpha} \partial u_{i\beta} \partial u_{i\gamma}} \right)_{\text{eq}} \langle u_{i\alpha} u_{i\gamma} \rangle + \frac{1}{3!} \sum_{\alpha, \gamma, \eta} \left( \frac{\partial^4 E_{ci}}{\partial u_{i\alpha} \partial u_{i\beta} \partial u_{i\gamma} \partial u_{i\eta}} \right)_{\text{eq}} \langle u_{i\alpha} u_{i\gamma} u_{i\eta} \rangle - \alpha_\beta = 0. \quad (7)$$

Here, the subscript eq indicates evaluation at equilibrium. The thermal averages of the atomic displacements  $\langle u_{i\alpha} u_{i\gamma} \rangle$  and  $\langle u_{i\alpha} u_{i\gamma} u_{i\eta} \rangle$  (called second- and third-order moments) at given site  $\mathbf{R}_i$  can be expressed in terms of the first moment  $\langle u_{i\alpha} \rangle$  with the aid of Eq. (5) as

$$\langle u_{i\alpha} u_{i\gamma} \rangle_a = \langle u_{i\alpha} \rangle_a \langle u_{i\gamma} \rangle_a + \theta \frac{\partial \langle u_{i\alpha} \rangle_a}{\partial \alpha_\gamma} + \frac{\hbar \delta_{\alpha\gamma}}{2m\omega} \coth\left(\frac{\hbar\omega}{2\theta}\right) - \frac{\theta \delta_{\alpha\gamma}}{m\omega^2}, \quad (8)$$

$$\langle u_{i\alpha} u_{i\gamma} u_{i\eta} \rangle_a = \langle u_{i\alpha} \rangle_a \langle u_{i\gamma} \rangle_a \langle u_{i\eta} \rangle_a + \theta P_{\alpha\gamma\eta} \langle u_{i\alpha} \rangle_a \frac{\partial \langle u_{i\gamma} \rangle_a}{\partial \alpha_\eta} + \theta^2 \frac{\partial^2 \langle u_{i\alpha} \rangle_a}{\partial \alpha_\gamma \partial \alpha_\eta} + \frac{\hbar \langle u_{i\eta} \rangle_a \delta_{\alpha\gamma}}{2m\omega} \coth\left(\frac{\hbar\omega}{2\theta}\right) - \theta \frac{\langle u_{i\eta} \rangle_a \delta_{\alpha\gamma}}{m\omega^2}. \quad (9)$$

Here,  $P_{\alpha\gamma\eta}$  is 1 ( $\alpha = \gamma = \eta$ ) or 0 (otherwise) depending on  $\alpha$ ,  $\gamma$ , and  $\eta$  (Cartesian component) and  $\omega$  is the atomic vibration frequency similar to that defined in the Einstein model, which will be given by Eq. (11). Then Eq. (7) is transformed into the new differential equation

$$\gamma_i \theta^2 \frac{d^2 y}{d\alpha^2} + 3\gamma_i \theta y \frac{dy}{d\alpha} + \gamma_i y^3 + k_i y + \gamma_i \frac{\theta}{k} (X \coth X - 1) y - \alpha_\beta = 0, \quad (10)$$

where  $X \equiv \hbar\omega/2\theta$  and  $y \equiv \langle u_i \rangle$ . Here,  $k_i$  and  $\gamma_i$  are second- and fourth-order derivatives of  $E_{ci}$  and defined by the following formulas:

$$k_i = \left( \frac{\partial^2 E_{ci}}{\partial u_{i\alpha}^2} \right)_{\text{eq}} \equiv m\omega^2, \quad (11)$$

$$\gamma_i = \frac{1}{6} \left[ \left( \frac{\partial^4 E_{ci}}{\partial u_{i\alpha}^4} \right)_{\text{eq}} + 6 \left( \frac{\partial^4 E_{ci}}{\partial u_{i\beta}^2 \partial u_{i\gamma}^2} \right)_{\text{eq}} \right] \equiv \frac{1}{6} (\gamma_{1i} + 6\gamma_{2i}), \quad (12)$$

respectively. In the SMA TB scheme, the parameters  $k_i$ ,  $\gamma_{1i}$ , and  $\gamma_{2i}$  are composed of two contributions (band structure and repulsive energies) and  $k_i$  is given by the following form:

$$k_i = \frac{q}{r_0} \left[ \eta_i^{(2)} - \left( 2 \frac{q}{r_0} \right) \eta_i^{(3)} \right] \mu_{2i}^{-1/2} - A(p/r_0) \sum_j \left[ \frac{1 - \ell_{ij}^2}{r_{ij}} - \ell_{ij}^2 \left( \frac{p}{r_0} \right) \right] \exp[-p(r_{ij}/r_0 - 1)], \quad (13)$$

where  $\eta_i^{(2)}$  and  $\eta_i^{(3)}$  are defined, respectively, as

$$\eta_i^{(2)} = \sum_j \left[ \frac{1 - l_{ij}^2}{r_{ij}} \right] \xi_{ij}^2 \exp[-2q(r_{ij}/r_0 - 1)], \quad (14)$$

$$\eta_i^{(3)} = \sum_j l_{ij}^2 \xi_{ij}^2 \exp[-2q(r_{ij}/r_0 - 1)], \quad (15)$$

with

$$l_{ij} = \left( \frac{\partial r_{ij}}{\partial x} \right) = (x_j - x_i)/r_{ij}.$$

After a bit of algebra,  $\gamma_{1i}$  defined by Eq. (12) is given by

$$\begin{aligned} \gamma_{1i} = & \left( \frac{q}{r_0} \right) \left[ \frac{\partial^2 \eta_i^{(2)}}{\partial x^2} - 2 \frac{\partial^2 \eta_i^{(3)}}{\partial x^2} \left( \frac{q}{r_0} \right) \right] \mu_{2i}^{-1/2} \\ & - \left( \frac{q}{r_0} \right)^2 \left[ \eta_i^{(2)} - 2 \eta_i^{(3)} \left( \frac{q}{r_0} \right) \right] \mu_{2i}^{-3/2} \\ & + A \left( \frac{p}{r_0} \right) \sum_j \left[ \frac{3(1 - 6l_{ij}^2 + 5l_{ij}^4)}{r_{ij}^3} \right. \\ & + \frac{3(1 - 6l_{ij}^2 + 5l_{ij}^4)}{r_{ij}^2} \left( \frac{p}{r_0} \right) - \frac{6l_{ij}^2}{r_{ij}} \left( \frac{p}{r_0} \right)^2 \\ & \left. + l_{ij}^4 \left( \frac{p}{r_0} \right)^4 \right] \exp\{-p(r_{ij}/r_0 - 1)\}. \quad (16) \end{aligned}$$

The second derivatives of  $\eta_i^{(2)}$  and  $\eta_i^{(3)}$  appearing in the first term of the right-hand side of Eq. (16) are also given explicitly in terms of the TB potential parameters and the direction cosines  $l_{ij}$  and  $m_{ij}$  between the central atom  $i$  and its neighboring atoms  $j$  (see Appendix B).  $\gamma_{2i}$  is expressed explicitly as

TABLE II. Lattice sums appearing in the harmonic  $k_1$  and anharmonic  $\gamma_1$  and  $\gamma_2$  parameters in cubic metals.  $\Sigma_1 \equiv \sum_{j \neq i} 1 - 6l_{ij}^2 + 5l_{ij}^4$ ,  $\Sigma_2 \equiv \sum_{j \neq i} 1 - 3l_{ij}^2 - 3m_{ij}^2 + 15l_{ij}^2 m_{ij}^2$ ,  $\Sigma_3 \equiv \sum_{j \neq i} l_{ij}^2 + m_{ij}^2 - 6l_{ij}^2 m_{ij}^2$ .

Crystal structure	Neighbors	1	2	3	4	5
fcc	$Z_i$	12	6	24	12	24
	Distance	1	$\sqrt{2}$	$\sqrt{3}$	2	$\sqrt{5}$
	$\sum_{j \neq i} l_{ij}^2$	4	2	8	4	8
	$\sum_{j \neq i} l_{ji}^4$	2	2	4	2	164/25
	$\sum_{j \neq i} l_{ij}^2 m_{ij}^2$	1	0	2	1	18/25
	$\sum_1$	-2	4	-4	-2	44/5
	$\sum_2$	3	-6	6	3	-66/5
$\sum_3$	2	4	4	2	292/25	
bcc	$Z_i$	8	6	12	24	8
	Distance	1	$2/\sqrt{3}$	$2\sqrt{6}/3$	$\sqrt{11}/3$	2
	$\sum_{j \neq i} l_{ij}^2$	8/3	2	4	8	8/3
	$\sum_{j \neq i} l_{ji}^4$	8/9	2	2	664/121	8/9
	$\sum_{j \neq i} l_{ij}^2 m_{ij}^2$	8/9	0	1	152/121	8/9
	$\sum_1$	-32/9	4	-2	416/121	-32/9
	$\sum_2$	16/3	-6	3	-624/121	16/3
$\sum_3$	0	4	2	1024/121	0	

$$\begin{aligned}
\gamma_{2i} = & \left( \frac{q}{r_0} \right) \left[ \frac{\partial^2 \eta_i^{(2)}}{\partial y^2} - 2 \frac{\partial^2 \eta_i^{(3)}}{\partial y^2} \left( \frac{q}{r_0} \right) \right] \mu_{2i}^{-1/2} - 2 \left[ \frac{\partial \eta_i^{(1)}}{\partial y} \right]^2 \left( \frac{q}{r_0} \right)^2 \mu_{2i}^{-3/2} + \left( \frac{q}{r_0} \right)^2 \left[ \eta_i^{(2)} - 2 \eta_i^{(3)} \left( \frac{q}{r_0} \right) \right]^2 \mu_{2i}^{-5/2} \\
& + A \left( \frac{p}{r_0} \right) \sum_j \left[ \frac{1 - 3l_{ij}^2 - 3m_{ij}^2 + 15l_{ij}^2 m_{ij}^2}{r_{ij}^3} + \frac{1 - 3l_{ij}^2 - 3m_{ij}^2 + 15l_{ij}^2 m_{ij}^2}{r_{ij}^2} \left( \frac{p}{r_0} \right) \right. \\
& \left. - \frac{l_{ij}^2 + m_{ij}^2 - 6l_{ij}^2 m_{ij}^2}{r_{ij}} \left( \frac{p}{r_0} \right)^2 + l_{ij}^2 m_{ij}^2 \left( \frac{p}{r_0} \right)^3 \right] \exp\{-p(r_{ij}/r_0 - 1)\}, \quad (17)
\end{aligned}$$

where  $\eta_i^{(1)}$  is defined by

$$\eta_i^{(1)} = \sum_j l_{ij} \xi_{ij}^2 \exp[-2q(r_{ij}/r_0 - 1)]. \quad (18)$$

Here, we note that  $\gamma_{1i}$  and  $\gamma_{2i}$  depend sensitively on the structure of crystals through factors including direction cosines as can be seen in Eqs. (16) and (17). The factors including direction cosines for cubic crystals are presented in Table II. The derivatives of  $\eta_i^{(1)}$ ,  $\eta_i^{(2)}$ , and  $\eta_i^{(3)}$  with respect to the  $y$  variable are given in Appendix B.

In determining the atomic displacement  $\langle u_i \rangle$ , the symmetry property appropriate for cubic crystals is used

$$\langle u_{i\alpha} \rangle = \langle u_{i\gamma} \rangle = \langle u_{i\eta} \rangle \equiv \langle u_i \rangle. \quad (19)$$

Then, the solutions of the nonlinear differential equation of Eq. (10) can be expanded in the power series of the supplemental force  $\alpha$  as

$$y = \Delta r + A_1 \alpha + A_2 \alpha^2. \quad (20)$$

Here,  $\Delta r$  is the atomic displacement in the limit of zero of supplemental force  $\alpha$ . Substituting the above solution of Eq.

(20) into the original differential equation Eq. (10), one can get the coupled equations on the coefficients  $A_1$  and  $A_2$ , from which the solution of  $\Delta r$  is given as

$$(\Delta r)^2 \approx [-C_2 + \sqrt{C_2^2 - 4C_1C_3}]/2C_1, \quad (21)$$

where

$$\begin{aligned} C_1 &= 3\gamma_i, \\ C_2 &= 3k_i \left[ 1 + \frac{\gamma_i \theta}{k_i^2} (X \coth X + 1) \right], \\ C_3 &= -\frac{2\gamma_i \theta^2}{k_i^2} \left( 1 + \frac{X \coth X}{2} \right). \end{aligned} \quad (22)$$

Using Eqs. (8) and (21), it can be shown that mean square atomic displacement (second moment) in cubic crystals is given by

$$\begin{aligned} \langle u^2 \rangle &= \frac{\theta}{k} X \coth X + \frac{2}{3} \frac{2\gamma\theta^2}{k^3} (1 + X \coth X/2) \\ &\quad + \frac{2\gamma^2\theta^3}{k^5} (1 + X \coth X)(1 + X \coth X/2). \end{aligned} \quad (23)$$

Once the thermal expansion  $\Delta r$  in the lattice is found, one can get the Helmholtz free energy of the system in the following form:

$$\Psi = U_0 + \Psi_0 + \Psi_1, \quad (24)$$

where  $\Psi_0$  denotes the free energy in the harmonic approximation and  $\Psi_1$  the anharmonicity contribution to the free energy.<sup>38–40</sup> We calculate the anharmonicity contribution to the free energy  $\Psi_1$  by applying the general formula

$$\Psi = U_0 + \Psi_0 + \int_0^\lambda \langle \hat{V} \rangle_\lambda d\lambda, \quad (25)$$

where  $\lambda \hat{V}$  represents the Hamiltonian corresponding to the anharmonicity contribution. It is straightforward to evaluate the following integrals analytically

$$I_1 = \int_0^{\gamma_1} \langle u_i^4 \rangle d\gamma_1, \quad I_2 = \int_0^{\gamma_2} \langle u_i^2 \rangle_{\gamma_1=0}^2 d\gamma_2. \quad (26)$$

Then the free energy of the system is given by

$$\begin{aligned} \Psi &= U_0 + 3N\theta [X + \ln(1 - e^{-2X})] \\ &\quad + 3N \left\{ \frac{\theta^2}{k^2} \left[ \gamma_2 X^2 \coth^2 X - \frac{2}{3} \gamma_1 \left( 1 + \frac{X \coth X}{2} \right) \right] \right. \\ &\quad + \frac{2\theta^3}{k^4} \left[ \frac{4}{3} \gamma_2^2 X \coth X \left( 1 + \frac{X \coth X}{2} \right) \right. \\ &\quad \left. \left. - 2\gamma_1(\gamma_1 + 2\gamma_2) \left( 1 + \frac{X \coth X}{2} \right) (1 + X \coth X) \right] \right\}, \end{aligned} \quad (27)$$

where the second term denotes the harmonic contribution to the free energy.

With the aid of the free energy formula  $\Psi = E - TS$ , one can find the thermodynamic quantities of metal systems. The specific heats and elastic moduli at temperature  $T$  are directly derived from the free energy  $\Psi$  of the system. For instance, the isothermal compressibility  $\chi_T$  is given by

$$\chi_T = 3(a/a_0)^3 \left/ \left[ 2P + \frac{1}{3N} \frac{\sqrt{2}}{a} \left( \frac{\partial^2 \Psi}{\partial r^2} \right)_T \right] \right., \quad (28)$$

where

$$\begin{aligned} \frac{\partial^2 \Psi}{\partial r^2} &= 3N \left\{ \frac{1}{6} \frac{\partial^2 U_0}{\partial r^2} + \theta \left[ \frac{X \coth X}{2k} \frac{\partial^2 k}{\partial r^2} \right. \right. \\ &\quad \left. \left. - \frac{1}{4k^2} \left( \frac{\partial k}{\partial r} \right)^2 \left( X \coth X + \frac{X^2}{\sinh^2 X} \right) \right] \right\}. \end{aligned} \quad (29)$$

On the other hand, the specific heats at constant volume  $C_v$  is

$$\begin{aligned} C_v &= 3Nk_B \left\{ \frac{X^2}{\sinh^2 X} + \frac{2\theta}{k^2} \left[ \left( 2\gamma_2 + \frac{\gamma_1}{3} \right) \frac{X^3 \coth X}{\sinh^2 X} \right. \right. \\ &\quad \left. \left. + \frac{\gamma_1}{3} \left( 1 + \frac{X^2}{\sinh^2 X} \right) - \gamma_2 \left( \frac{X^4}{\sinh^4 X} + \frac{2X^4 \coth^2 X}{\sinh^2 X} \right) \right] \right\}. \end{aligned} \quad (30)$$

The specific heat at constant pressure  $C_p$  is determined from the thermodynamic relations

$$C_p = C_v + \frac{9TV\alpha_T^2}{\chi_T}, \quad (31)$$

where  $\alpha_T$  denotes the linear thermal expansion coefficient and  $\chi_T$  the isothermal compressibility. In Eqs. (27), (29), and (30) above, the suffices  $i$  for the parameters  $k$ ,  $\gamma_1$  and  $\gamma_2$  are omitted because each atomic site is equivalent in a monoatomic cubic crystal with primitive structure. The relationship between the isothermal and adiabatic compressibilities,  $\chi_T$  and  $\chi_s$ , is simply given by

$$\chi_s = \frac{C_v}{C_p} \chi_T. \quad (32)$$

One can also find “thermodynamic” Grüneisen constant as

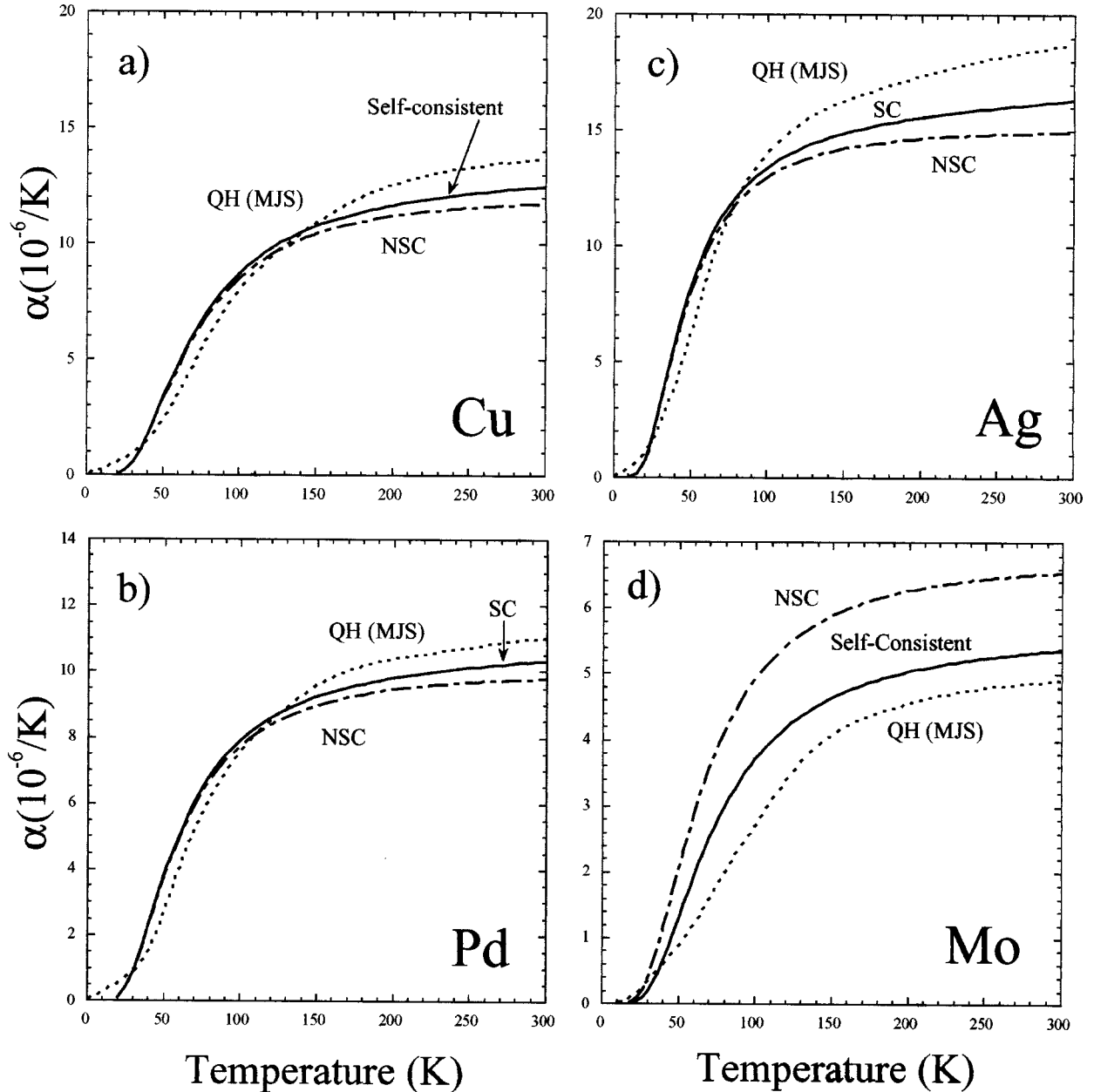


FIG. 1. Comparison of linear thermal expansion coefficients  $\alpha_T$  of (a) Cu, (b) Pd, (c) Ag, and (d) Mo, calculated by using the Morse potentials. Solid and dot-dashed lines show the results of self-consistent (SC) and non-self-consistent (NSC) treatments of the statistical moment method, respectively, while the dashed ones are the results of the QH theory by Moruzzi, Janak, and Schwarz (MJS).

$$\gamma_G = \frac{V}{C_v} \left[ \frac{\partial S}{\partial V} \right]_T = \frac{\alpha_T B_S V}{C_P}, \quad (33)$$

where  $B_S \equiv \chi_S^{-1}$  denotes the adiabatic bulk modulus.

### III. RESULTS AND DISCUSSIONS

#### A. Comparison with the quasiharmonic theory

Firstly, we compare the thermodynamic quantities of metals calculated by the present statistical moment method (SMM) with those by the QH theory.<sup>10</sup> The basic idea of the QH approximation is that the explicit dependence of the free

energy  $F(T, V)$  on the system volume  $V$  can be explored by homogeneous scaling of the atomic potentials  $\{R_i^0\}$ . Then, for each temperature  $T$  the equilibrium volume  $V$  is obtained by minimizing Helmholtz energy  $F$  with respect to  $V$ . In Fig. 1, we present the linear thermal expansion coefficients  $\alpha_T$  of Cu, Pd, Ag, and Mo metals, calculated by the present theory, together with those of the QH theory by Moruzzi, Janak, and Schwarz (MJS model).<sup>10</sup> The linear thermal expansion coefficients  $\alpha_T$  by the present statistical moment theory and those of the QH theory by Moruzzi *et al.* are referred to as SMM and MJS, respectively. In order to allow the direct comparison between the two different schemes, the linear thermal expansion coefficients  $\alpha_T$  of the cubic metals are calculated

with the use of the same Morse type of potentials, exactly identical forms as used in the QH calculations by MJS.<sup>10</sup> The four metals Cu, Pd, Ag, and Mo are chosen simply because the linear thermal expansion coefficients  $\alpha_T$  are well reproduced by the two-body Morse potentials as demonstrated by them.<sup>10</sup>

The solid lines in Fig. 1 show the linear thermal expansion coefficients  $\alpha_T$  calculated by the self-consistent (SC) treatments of the present SMM scheme, while the dot-dashed ones are obtained by the non-self-consistent (NSC) treatments. In the SC treatments, the characteristic parameters  $k$ ,  $\gamma_1$ , and  $\gamma_2$  are determined self-consistently with the lattice constants  $a_T$  at given temperature  $T$ . However, in the NSC treatments, the harmonic  $k$ , and anharmonic  $\gamma_1$ , and  $\gamma_2$  parameters are fixed to those values evaluated at the appropriate reference temperature  $T_0$  (e.g., absolute zero temperature or some reference temperature; here  $T_0$  is chosen to be 0 K and taken to be constant for the whole temperature region). The calculated linear thermal expansion coefficients  $\alpha_T$  by the present theory are in good agreement with those by QH theory for the lower temperature region below the Debye temperature and the agreement is better for the SC calculations. This indicates that the thermal lattice expansion gives rise to the significant reduction in the parameters  $k$ ,  $\gamma_1$ , and  $\gamma_2$ , and thereby changes the thermodynamic quantities appreciably even for the lower temperatures.

### B. Thermodynamic quantities of metals by second moment TB potentials

With the use of the analytic expressions presented in Sec. II, it is straightforward to calculate the thermodynamic quantities of metals and alloys at the thermal equilibrium. Firstly, the equilibrium lattice spacings are determined, using Eqs. (20) and (21), in the SC treatment including temperature (bond length) -dependent  $k$ ,  $\gamma_1$ , and  $\gamma_2$  values. The thermal lattice expansion can also be calculated by standard procedure of minimizing the Helmholtz energy of the system: We have checked that both calculations give almost identical results on the thermal lattice expansions. We calculate the thermal lattice expansion and mean-square atomic displacements of some fcc (transition) metals and bcc alkali metals, for which the reliable many-body potentials are available, and compare them with those by the molecular dynamics (MD) and Monte Carlo (MC) simulations. So far, a number of the SMA base TB potentials have been proposed for fcc metals. Specifically, we use the SMA TB potentials by Rosato *et al.*<sup>35</sup> and by Cleri and Rosato<sup>36</sup> for fcc metals, which are known to give good descriptions of cohesive properties of fcc elements. For alkali metals Li, Na, K, Rb, and Cs, we use the potential parameters proposed recently by Li *et al.*<sup>40</sup>

In the TB scheme by Rosato *et al.*,<sup>35</sup> the interaction range is limited to the first nearest neighbors, while in the TB scheme by Cleri and Rosato,<sup>36</sup> it is extended to the fifth neighbors. In Fig. 2, we present the linear thermal expansion coefficients  $\alpha_T$  and mean-square atomic displacements  $\langle u^2 \rangle$  of Cu crystal, together with the experimental values (by symbols  $\circ$ ).<sup>55-58</sup> For this calculation, the electronic many-body potentials are used for Cu crystal, but there are no large

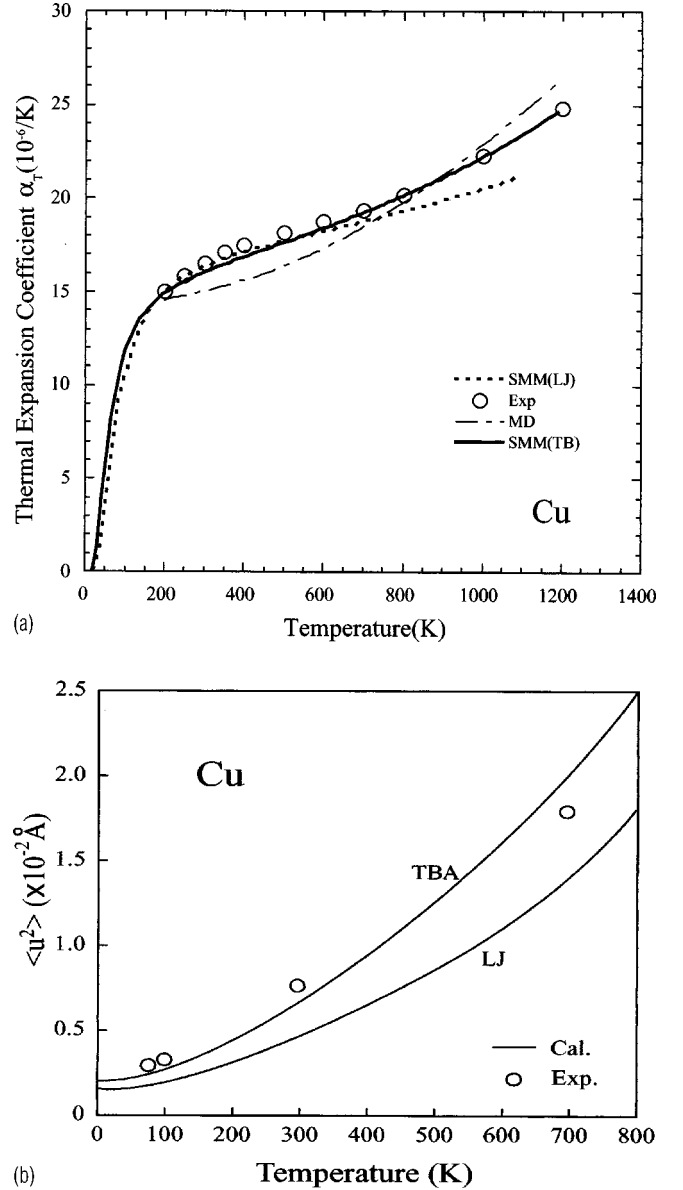


FIG. 2. (a) The linear thermal expansion coefficient  $\alpha_T$  (a) and (b) mean-square atomic displacements  $\langle u^2 \rangle$  of Cu crystal calculated by the present method. The corresponding experimental values are presented by symbols  $\circ$ .

differences in the calculated quantities when we use the Lennard-Jones (LJ) type of pair potentials. The bold line in Fig. 2(a) represents the calculated  $\alpha_T$  by the present SMM, while the dashed line  $\alpha_T$  values by the Lennard-Jones type of potential;  $\varphi(r) = D_0 \left\{ (r_0/r)^n - (n/m)(r_0/r)^m \right\}$ , with  $n = 9.0$ ,  $m = 5.5$ ,  $r_0 = 2.5487 \text{ \AA}$ , and  $D_0 = 4125.7 \text{ K}$  (0.35553 eV), respectively. The overall agreement between the calculated and experimental  $\alpha_T$  values is better for the calculations by the SMA TB potential, although LJ potential parameters are not best fitted to reproduce the experimental  $\alpha_T$  values. We note that the classical MD simulation,<sup>59</sup> shown by the dot-dashed curve in Fig. 2(a), do not reproduce the correct curvature of the linear thermal expansion coefficient  $\alpha_T$ , and is qualitatively incorrect due to the absence of the quan-

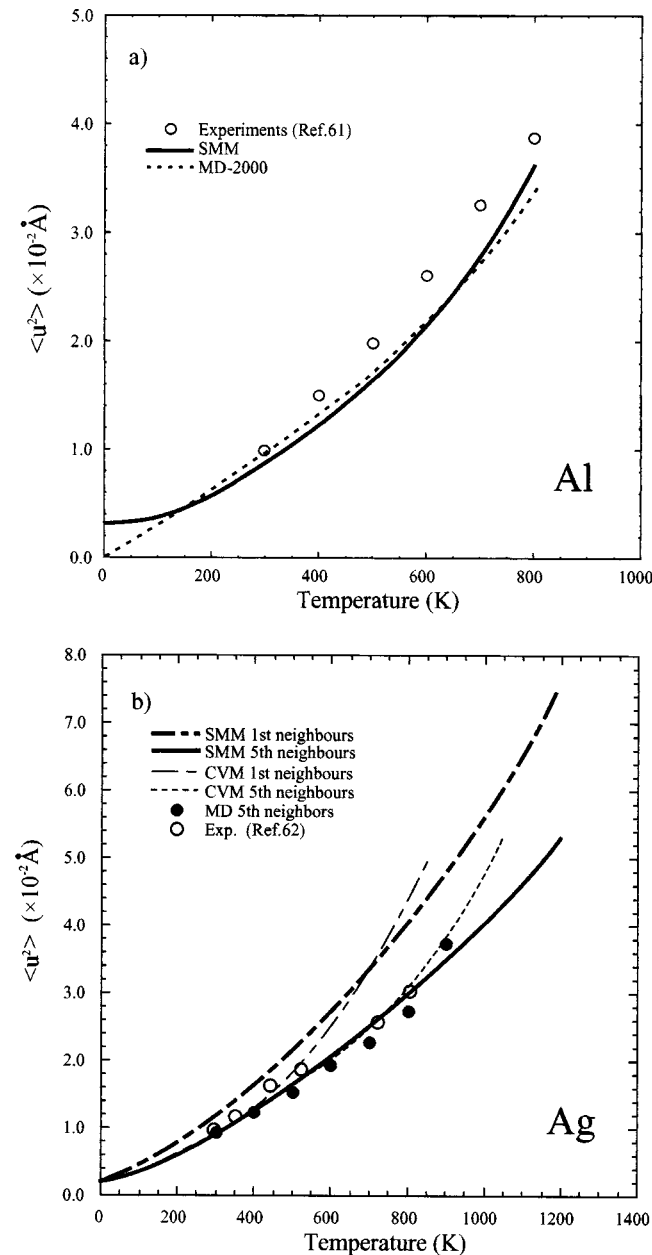


FIG. 3. Mean-square atomic displacements  $\langle u^2 \rangle$  of (a) Al and (b) Ag crystals as a function of temperature. In (a), the dashed line shows the results of MD simulations by Papanicolaou *et al.* (Ref. 60), while the solid circles are the experimental values.

tum mechanical vibration effects. One also sees in Fig. 2(b) that the agreements between the calculated and experimental results of the mean square atomic displacements  $\langle u^2 \rangle$  in Cu crystal are quite excellent for the SMA TB calculations, compared to those by two-body potentials. This implies that the present SMM scheme with SMA TB potentials provides us fully quantitative estimates for the thermodynamic quantities of elemental metals.

We show in Fig. 3(a) the mean-square atomic displacements  $\langle u^2 \rangle$  of Al crystal as a function of temperature  $T$ , together with those values by the MD simulation<sup>60</sup> and experimental data.<sup>61</sup> The present calculations by using SMM

differ significantly from those results by MD simulations, especially for the lower temperature region, i.e., below the Debye temperature. This is due to the fact that in the classical MD simulations the quantum mechanical vibration effects are not taken into account. One sees that the quantum mechanical zero point vibrations give main contributions at lower temperature region  $T \leq 100$  K. The agreement between the present calculation and the experimental results is fairly good for the whole temperature region, from zero to  $\sim 800$  K, much higher than the Debye temperature. In Fig. 3(b), we show the mean-square atomic displacements  $\langle u^2 \rangle$  of Ag crystal calculated by the present SMM using the SMA TB potentials of Refs. 35 and 36, together with the experimental results.<sup>62</sup> One sees in Fig. 3(b) that TB parameters by Rosato, Guillope, and Legrand<sup>35</sup> (first-neighbor TB potential) leads to larger mean-square atomic displacement  $\langle u^2 \rangle$  in Ag crystal compared to those results by using the TB parameters by Cleri and Rosato<sup>36</sup> (5th neighbor TB potential). The similar tendency is also found for the thermal expansion coefficients  $\alpha_T$  of Ag crystal, larger  $\alpha_T$  values by TB potential by Rosato, Guillope, and Legrand.<sup>35</sup> In the present formalism, the thermal lattice expansion and mean-square atomic displacements are characterized by the harmonic  $k$  and anharmonic  $\gamma$  parameters. In particular, the thermal lattice expansion (material dependence) is predicted by a ratio of  $\gamma/k^2$  and the mean-square displacement  $\langle u^2 \rangle$  by  $\gamma/k^2$  (and also by  $\gamma^2/k^5$ ) parameter as well. The ratios  $\gamma/k^2$  of Cu crystal calculated by using the TB potential by Rosato, Guillope, and Legrand<sup>35</sup> are in fact larger than those results by Cleri and Rosato<sup>36</sup> for whole temperature region. The mean square atomic displacement  $\langle u^2 \rangle$  in Ag crystal by the fifth-neighbor TB potential<sup>36</sup> are in fairly good agreement with the experimental results for the whole temperature region, and they are in good agreement with the MD simulation results for high temperature region.

The calculated mean-square atomic displacements  $\langle u^2 \rangle$  of Ag crystal by the present method is also compared with those by the cluster variation method (CVM). As is well known, CVM<sup>63–65</sup> is an analytical statistical method that directly gives us the free energy of a system. The CVM was originally designed for the statistical mechanics of the Ising model on a fixed lattice, and extended recently to treat systems with continuous degrees of freedom, such as the lattice site distortion, due to thermal vibrations, thermal dilatation, and mixture of atoms of different sizes. In general, in CVM treatments the correlations in the atomic displacements are taken into account within the small atomic clusters (e.g., small clusters such as pair, tetrahedron, or octahedron clusters). Finel and Tétot gave the first application of the Gaussian CVM<sup>65</sup> for the thermodynamic quantities of some transition metals. It has been demonstrated that Gaussian CVM gives the excellent results of the thermodynamic quantities of metals (the CPU time is several orders of magnitude smaller than the one needed for numerical MD or MC simulations). The thin dot-dashed and thin dashed curves in Fig. 3(b) represent the mean-square atomic displacement  $\langle u^2 \rangle$  of Ag crystal obtained by the Gaussian CVM<sup>65</sup> using the SMA TB potentials of Refs. 35 and 36, respectively. Both CVM

TABLE III. Bulk modulus, linear thermal expansion, and Grüneisen constant calculated with the use of the SMA TB potentials. Experimental values of Na\*(RT) are those values for 250 K.

Element	$B_T(\text{GPa})$			$\alpha (10^{-6} \text{ K}^{-1})$		$\gamma_G$	
	Calc.			Calc.	Expt.	Calc.	Expt.
	$T=0$	RT	Expt.				
Al	87	75	72	24.5	23.6	2.09	2.19
Cu	153	137	137	15.9	16.7	2.21	2.00
Ni	190	182	184	14.7	12.7	2.01	1.88
Ag	114	96	101	23.5	19.7	2.78	2.36
Rh	306	280	271	10.9	8.2	2.19	2.43
Pd	204	171	181	14.3	11.6	2.22	2.18
Au	185	164	173	17.2	14.2	3.21	3.04
Pt	301	259	278	11.2	8.9	3.06	2.56
Li	16.8	12.4	11.6	65.4	56.0	1.18	1.18
Na*	6.5	4.3	6.8	83.9	71.0	1.53	1.31
K	5.3	3.6	3.2	98.7	83.0	1.54	1.37
Rb	4.0	2.8	3.1	104.6	90.0	1.65	1.67
Cs	2.9	2.1	2.0	108.8	97.0	1.55	1.44

calculations of  $\alpha_T$  are generally in agreement with the experimental results. We note that for  $\langle u^2 \rangle$  calculations of Ag crystal, however, the present analytic SMM gives much efficient analytic calculations and much better results compared to those by CVM calculations.

The calculated thermodynamic quantities of cubic metals, fcc (in addition to Cu, Ag, and Al presented above) and alkali (bcc) metals, by the present method are summarized in Table III. In the present calculations, we use the TB potential parameters by Li, Barojas, and Papaconstantopoulos<sup>40</sup> for alkali metals Li, Na, K, Rb, and Cs. This TB model takes into account the interatomic interactions up to 12th neighbors, i.e., 228 atoms in bcc lattice. The relative magnitudes of linear thermal expansion coefficients of fcc (transition) metals are in good agreement with the experimental results. However, the thermal lattice expansion coefficients  $\alpha$  of alkali metals are systematically larger ( $\sim 10\%$ ) than those of experimental results, although their relative magnitudes are in good agreement with the experimental results. The calculated Grüneisen constants and elastic moduli are also presented in Table III. The anharmonicity of the lattice vibrations is well described by the Grüneisen constant  $\gamma_G$ . The material of larger value of  $\gamma_G$  may be regarded as the material with higher lattice anharmonicity. So, the evaluation of the Grüneisen constant is of great significance for the assessment of anharmonic thermodynamic properties of metals and alloys. The experimental Grüneisen constants  $\gamma_G$  of fcc metals are larger than 2 except for Ni, while those of alkali metals are less than 2 and take values around  $\sim 1.5$ . The calculated Grüneisen constants  $\gamma_G$  of fcc metals are also larger than 2, while those values of alkali metals are less than 2, in agreement with the experimental results. The calculated  $\gamma_G$  values by the present method have the weak temperature dependence, i.e., show the slight increase with increasing temperature as in the calculations by QH theory.<sup>10</sup> The tabu-

lated Grüneisen constants  $\gamma_G$  for low temperatures are well compared with the experimental values which are deduced from the low (room-) temperature specific heats.

The lattice specific heats  $C_v$  and  $C_p$  at constant volume and at constant pressure are calculated using Eqs. (30) and (31), respectively. However, the evaluations by Eqs. (30) and (31) are the lattice contributions, and their values may not be directly compared with the corresponding experimental values. We do not include the contributions of lattice vacancies and electronic parts of the specific heats  $C_v$ , which are known to give significant contributions in metals for higher temperature region near the melting temperature. In particular, it has been demonstrated that lattice vacancies make a large contribution to the specific heats for the high-temperature region.<sup>66</sup> The electronic contribution to the specific heat at constant volume  $C_v^{\text{ele}}$  is proportional to the temperature  $T$  and given by  $C_v^{\text{ele}} = \gamma_e T$ ,  $\gamma_e$  being the electronic specific heat constant.<sup>56,66</sup> The electronic specific heats  $C_v^{\text{ele}}$  values are estimated to be 0.8–13.4% of  $C_v^{\text{lat}}$  for metals considered here by the free-electron model.<sup>56</sup> Therefore, the present formulas of the lattice contribution to the specific heats, both  $C_v$  and  $C_p$ , for the cubic metals tend to underestimate the specific heats for higher temperature region, when compared with the experimental results. The lattice contribution of specific heats  $C_p$  calculated for Cu crystal is shown in Fig. 4, together with the experimental results<sup>58</sup> and those of MD simulation results. As expected from above mentioned reasonings, the calculated  $C_p$  values of solid Cu are smaller than the experimental values at high temperatures. However, the temperature dependence (curvature) of  $C_p$  of Cu crystal by the present method is in good agreement with the experimental results, in contrast to the MD simulation results. In the MD simulations, the heat capacities per atom at constant pressure  $C_p$  can be obtained for metals by

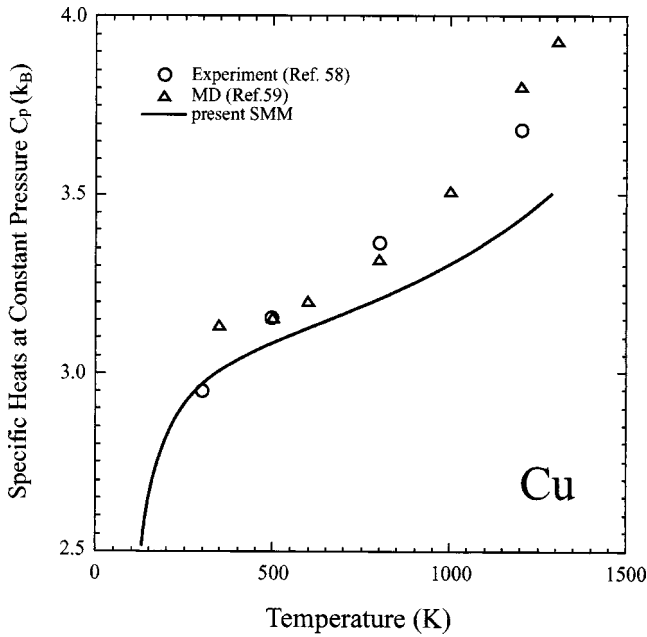


FIG. 4. Specific heats per atom at constant pressure  $C_p$  plotted against temperature  $T$  for Cu crystal, in unit of Boltzmann's constant  $k_B$ . The experimental data (Ref. 58) are shown as the open circles.

taking the numerical derivative of the internal energy with respect to temperature.<sup>59</sup> The MD simulations by Mei, Davenport, and Fernando<sup>59</sup> give reasonable values of  $C_p$  for higher temperature region when compared with the experimental data. However, it should be noted that the MD simulations are only adequate above the room temperature, and the calculated  $C_p$  value deviates from the experimental data at low temperatures because quantum effects are not taken into account in the classical MD simulations.

The bulk moduli  $B_T$  of cubic metals are evaluated at absolute zero temperature and at room temperature (RT) and presented also in Table III. The ratios of bulk moduli,  $B_T/B_0$ , with respect to those of the absolute zero temperature are calculated to be 0.85–0.90 (fcc metals) and  $\sim 0.7$  (alkali metals) which are favorably compared with the experimental results. In general, the calculated bulk moduli  $B_T(\text{RT})$  and  $B_0$  are in good agreement with the experimental results as well as QH calculations.

As a final remark of this section, we note that the present statistical moment method can be incorporated in a straightforward manner with the first-principles density functional theory, by simply evaluating three kinds of derivatives (one for harmonic and two for anharmonic contributions) of the atomic total energy with respect to the Cartesian coordinates. The density functional TB<sup>67</sup> and TBTE<sup>68</sup> (tight-binding total energy) methods with Slater-Koster parameters derived from the first-principles theories can be readily applied to evaluate  $k$ ,  $\gamma_1$ , and  $\gamma_2$  values, on the basis of Hellman-Feynman theorem. The full density functional theories such as the linear-response approach by Giannozzi *et al.*<sup>69</sup> and real-space finite-element density matrix method<sup>70</sup> can also be used for

the evaluations of  $k$ ,  $\gamma_1$ , and  $\gamma_2$ , and thus for the calculations of thermodynamic quantities of the present study.

#### IV. CONCLUSIONS

We have presented an analytic formulation for obtaining the thermodynamic quantities of metals and alloys based on the finite temperature moment expansion technique in the statistical physics. The thermal lattice expansion of monatomic crystals (fourth-order anharmonic contribution) is derived explicitly in terms of the three characteristic parameters,  $k_1$ ,  $\gamma_1$ , and  $\gamma_2$ . The present formalism takes into account the quantum-mechanical zero-point vibrations as well as the higher-order anharmonic terms in the atomic displacements and it enables us to derive the various thermodynamic quantities of metals and alloys for a wide temperature range. We are able to calculate the thermodynamic quantities quite efficiently and accurately by using the analytic formulas and taking into account the many-body electronic effects in metallic systems. The calculated thermodynamic quantities of metals are in good agreement with the experimental results as well as with those by MD and MC simulations (in some cases, better results by the present method).

Although in this paper we only used many-body electronic potentials, the extension to coupling the present SMM scheme with the *ab initio* density functional theories is straightforward. This can be done by evaluating three characteristic parameters  $k$ ,  $\gamma_1$ , and  $\gamma_2$  for cubic systems. It can also be applied directly for the composition-temperature phase diagrams calculations of alloys for the full temperature range from absolute zero to the melting temperatures  $T_m$ .

#### ACKNOWLEDGMENTS

The authors would like to thank Professor S. Tsuneyuki of Institute for Solid State Physics of the University of Tokyo for valuable discussions. The support of the supercomputing facility of Institute for Solid State Physics, the University of Tokyo is also acknowledged.

#### APPENDIX A: MOMENT DEVELOPMENT BY DENSITY MATRIX FORMALISM

To derive the mean-square atomic displacement (second moment) and higher-order power moments of the thermal lattice vibrations, we use the formalism based on the density matrix  $\hat{\rho}$ , which is defined by

$$\hat{\rho} = \exp\left(\frac{\Psi - \hat{H}}{\theta}\right), \quad (\text{A1})$$

where  $\Psi$  and  $\hat{H}$  denote the Helmholtz free energy and Hamiltonian of the system, respectively. In the presence of the constant supplemental forces  $\alpha_1, \alpha_2, \dots, \alpha_N$  in the system, the Hamiltonian  $\hat{H}$  is given by  $\hat{H} = \hat{H}_0 - \sum_i \alpha_i \hat{q}_i$ . The density matrix  $\hat{\rho}$  is normalized so as to satisfy the condition  $\text{Tr} \hat{\rho} = 1$  and given by the solution of the Liouville equation

$$i\hbar \frac{\partial \hat{\rho}}{\partial t} = [\hat{H}, \hat{\rho}]_- . \quad (\text{A2})$$

We use the following identities on the derivatives of an operator function  $\hat{E}_\lambda$  composed of two different operators  $\hat{A}$  and  $\hat{B}$ :

$$\hat{E}_\lambda(\tau, \hat{A}, \hat{B}) \equiv \exp[\tau(\hat{A} + \lambda \hat{B})] \quad (\text{A3})$$

$$\begin{aligned} \frac{\partial \hat{E}_\lambda(\tau, \hat{A}, \hat{B})}{\partial \lambda} &= \left\{ \tau \hat{B} + \sum_{n=1}^{\infty} \frac{\tau^{n+1} (i\hbar)^n}{(n+1)!} [\hat{A} + \lambda \hat{B} [\hat{A} + \lambda \hat{B} \dots [\hat{A} \right. \\ &\quad \left. + \lambda \hat{B} \dots]]] \right\} \hat{E}_\lambda(\tau, \hat{A}, \hat{B}) \\ &= \hat{E}_\lambda(\tau, \hat{A}, \hat{B}) \left\{ \tau \hat{B} - \sum_{n=1}^{\infty} \frac{(-\tau)^{n+1} (i\hbar)^n}{(n+1)!} \right. \\ &\quad \left. \times [\hat{A} + \lambda \hat{B} [\hat{A} + \lambda \hat{B} \dots [\hat{A} + \lambda \hat{B} \dots]]] \right\}, \quad (\text{A4}) \end{aligned}$$

$$\text{where } [\hat{A} + \lambda \hat{B}, \hat{B}] = \frac{1}{i\hbar} \{(\hat{A} + \lambda \hat{B})\hat{B} - \hat{B}(\hat{A} + \lambda \hat{B})\}.$$

By differentiation of the density matrix  $\hat{\rho}$  with respect to the constant force  $\alpha_i$ , one can get the relation

$$\frac{1}{\theta} \frac{\partial \Psi}{\partial \alpha_i} + \frac{1}{\theta} \left[ -\langle \hat{q}_i \rangle_a - \sum_{n=1}^{\infty} \frac{1}{(n+1)!} \left( \frac{i\hbar}{\theta} \right)^n \langle \hat{q}_i^{(n)} \rangle_a \right] = 0, \quad (\text{A5})$$

where

$$\langle \hat{q}_i^{(n)} \rangle = \text{Tr}[\dots [\hat{q}_i, \hat{H}]_- \hat{H} \dots] \hat{\rho}. \quad (\text{A6})$$

For equilibrium state, one can show that  $\langle \hat{q}_i^{(n)} \rangle = 0$  because  $\partial \hat{\rho} / \partial t = [\hat{H}, \hat{\rho}]_- = 0$  is satisfied. One can then derive from (A5) the relation

$$\langle \hat{q}_k \rangle_a = \frac{\partial \Psi}{\partial \alpha_k}. \quad (\text{A7})$$

Using the relation  $\langle \hat{F} \rangle_a = \text{Tr}[\hat{F} \hat{\rho}]$  and Eqs. (A3) and (A4), one can get the following identities:

$$\begin{aligned} \langle (\hat{F} - \langle \hat{F} \rangle) (\hat{q} - \langle \hat{q} \rangle) \rangle &= -\theta \left( \frac{\partial \langle \hat{F} \rangle}{\partial \alpha} - \left\langle \frac{\partial \hat{F}}{\partial \alpha} \right\rangle \right) \\ &\quad + \theta \sum_{m=1}^{\infty} (-1)^m \frac{B_m}{m!} \left( \frac{i\hbar}{\theta} \right)^m \left\langle \frac{\partial \hat{F}^{(m)}}{\partial \alpha} \right\rangle, \quad (\text{A8}) \end{aligned}$$

$$\begin{aligned} &\langle (\hat{q} - \langle \hat{q} \rangle) (\hat{F} - \langle \hat{F} \rangle) \rangle \\ &= -\theta \left( \frac{\partial \langle \hat{F} \rangle}{\partial \alpha} - \left\langle \frac{\partial \hat{F}}{\partial \alpha} \right\rangle \right) \\ &\quad + \theta \sum_{m=1}^{\infty} (-1)^m \frac{B_m}{m!} \left( -\frac{i\hbar}{\theta} \right)^m \left\langle \frac{\partial \hat{F}^{(m)}}{\partial \alpha} \right\rangle. \quad (\text{A9}) \end{aligned}$$

Then, one gets the decoupling formula

$$\begin{aligned} &\frac{1}{2} \langle [\hat{F}, \hat{q}_k]_+ \rangle_a - \langle \hat{F} \rangle_a \langle \hat{q}_k \rangle_a \\ &= \theta \frac{\partial \langle \hat{F} \rangle_a}{\partial \alpha_k} - \theta \sum_{n=0}^{\infty} \frac{B_{2n}}{(2n)!} \left( \frac{i\hbar}{\theta} \right)^{2n} \left\langle \frac{\partial \hat{F}^{(2n)}}{\partial \alpha_k} \right\rangle_a, \quad (\text{A10}) \end{aligned}$$

In the above Eqs. (A8)–(A10),  $B_{2n}$  denotes the Bernoulli number and  $\hat{F}^{(k)}$  is defined by

$$\hat{F}^{(k)} = \frac{1}{(i\hbar)^k} [\dots [\hat{F}, \underbrace{\hat{H}}_k \dots]_- \hat{H}]_- . \quad (\text{A11})$$

Substituting  $\hat{F} = \hat{q}_k$  into Eq. (A10), one can get the mean-square atomic displacement from the thermal equilibrium position, as

$$\langle (\hat{q}_i - \langle \hat{q}_i \rangle_a)^2 \rangle_a = \theta \frac{\partial \langle \hat{q}_i \rangle_a}{\partial \alpha_i} - \theta \sum_{n=0}^{\infty} \frac{B_{2n}}{(2n)!} \left( \frac{i\hbar}{\theta} \right)^{2n} \left\langle \frac{\partial \hat{q}_i^{(2n)}}{\partial \alpha_i} \right\rangle_a. \quad (\text{A12})$$

Equation (A12) is used to derive Eq. (8) in the text. The similar formulas can be given for higher order moments as well.

## APPENDIX B: DERIVATIVES OF COUPLING PARAMETERS $\mathbf{k}$ AND $\gamma$

The second derivatives such as  $\partial^2 \eta_i^{(2)} / \partial x^2$  and  $\partial^2 \eta_i^{(3)} / \partial x^2$ , appearing in Eq. (16) in the text are given by the following forms, respectively:

$$\begin{aligned} \frac{\partial^2 \eta_i^{(2)}}{\partial x^2} &= \sum_j \left[ -3(1 - 6l_{ij}^2 + 5l_{ij}^4) r_{ij}^{-3} \right. \\ &\quad \left. - 2(1 - 8l_{ij}^2 + 7l_{ij}^4) r_{ij}^{-2} \left( \frac{q}{r_0} \right) \right. \\ &\quad \left. + 4l_{ij}^2 (1 - l_{ij}^2) r_{ij}^{-1} \left( \frac{q}{r_0} \right)^2 \right] \xi_{ij}^2 \exp[-2q(r_{ij}/r_0 - 1)], \quad (\text{B1}) \end{aligned}$$

$$\frac{\partial^2 \eta_i^{(3)}}{\partial x^2} = \sum_j \left[ 2(1 - 5l_{ij}^2 + 4l_{ij}^4)r_{ij}^{-2} + 10l_{ij}^2(1 - l_{ij}^2)r_{ij}^{-1} \left( \frac{q}{r_0} \right) + 4l_{ij}^4 \left( \frac{q}{r_0} \right)^2 \right] \xi_{ij}^2 \exp[-2q(r_{ij}/r_0 - 1)]. \quad (\text{B2})$$

On the other hand, the first and second derivatives such as  $\partial \eta_i^{(1)}/\partial y$ ,  $\partial^2 \eta_i^{(2)}/\partial y^2$ , and  $\partial^2 \eta_i^{(3)}/\partial y^2$  with respect to the  $y$  variable are given by

$$\frac{\partial^2 \eta_i^{(1)}}{\partial y} = \sum_j \left[ l_{ij} m_{ij} \cdot r_{ij}^{-1} + 2l_{ij} m_{ij} \left( \frac{q}{r_0} \right) \right] \xi_{ij}^2 \times \exp[-2q(r_{ij}/r_0 - 1)], \quad (\text{B3})$$

$$\frac{\partial^2 \eta_i^{(2)}}{\partial y^2} = - \sum_j \left[ (1 - 3l_{ij}^2 - 3m_{ij}^2 + 15l_{ij}^2 m_{ij}^2) r_{ij}^{-3} + 2(1 - 3m_{ij}^2 - l_{ij}^2 + 7l_{ij}^2 m_{ij}^2) r_{ij}^{-1} \left( \frac{q}{r_0} \right) - 4(m^2 - l^2 m^2) r_{ij}^{-1} \left( \frac{q}{r_0} \right)^2 \right] \xi_{ij}^2 \times \exp[-2q(r_{ij}/r_0 - 1)], \quad (\text{B4})$$

and

$$\frac{\partial^2 \eta_i^{(3)}}{\partial y^2} = \sum_j \left[ -2(l_{ij}^2 - 4l_{ij}^2 m_{ij}^2) r_{ij}^{-2} - 2l_{ij}^2 (1 - 5m_{ij}^2) r_{ij}^{-1} \left( \frac{q}{r_0} \right) + 4l_{ij}^2 m_{ij}^2 \left( \frac{q}{r_0} \right)^2 \right] \xi_{ij}^2 \times \exp[-2q(r_{ij}/r_0 - 1)], \quad (\text{B5})$$

respectively.

- <sup>1</sup>P. E. A. Turchi and A. Gonis, *Statics and Dynamics of Alloy Phase Transformations* (Plenum, New York, 1994), p. 345.
- <sup>2</sup>*Foundations and Applications of Cluster Variation Method and Path Probability Method*, edited by T. Morita, M. Suzuki, K. Wada, and M. Kaburagi, *Suppl. Prog. Theor. Phys.* **115**, 1 (1994).
- <sup>3</sup>J. L. Morán-López and J. M. Sanchez, *Theory and Applications of the Cluster Variation and Path Probability Methods* (Plenum, New York, 1996).
- <sup>4</sup>R. Ahuja, J. M. Wills, B. Johansson, and O. Eriksson, *Phys. Rev. B* **48**, 16 269 (1993).
- <sup>5</sup>S. A. Ostanin and V. Yu. Trubitsin, *Phys. Rev. B* **57**, 13 485 (1998).
- <sup>6</sup>U. Pinsook and G. J. Ackland, *Phys. Rev. B* **58**, 11 252 (1998); **59**, 13 642 (1999).
- <sup>7</sup>A. Zupan, P. Blaha, K. Schwarz, and J. P. Perdew, *Phys. Rev. B* **58**, 11 266 (1998).
- <sup>8</sup>P. J. Wojtowaz and J. G. Kirkwood, *J. Chem. Phys.* **33**, 1299 (1960).
- <sup>9</sup>M. Asta, R. McCormark, and D. de Fontaine, *Phys. Rev. B* **93**, 748 (1993).
- <sup>10</sup>V. L. Moruzzi, J. F. Janak, and K. Schwarz, *Phys. Rev. B* **37**, 790 (1988).
- <sup>11</sup>A. P. Sutton, *Philos. Mag. A* **60**, 147 (1989).
- <sup>12</sup>V. Ozolins, C. Wolrerton, and A. Zunger, *Phys. Rev. B* **57**, 4816 (1998); **57**, 6427 (1998); **58**, R5897 (1998).
- <sup>13</sup>K. Persson, M. Ekman, and G. Grimvall, *Phys. Rev. B* **60**, 9999 (1999).
- <sup>14</sup>V. Ozolins and M. Asta, *Phys. Rev. Lett.* **86**, 448 (2001).
- <sup>15</sup>Van de Walle and G. Ceder, *Rev. Mod. Phys.* **74**, 11 (2002).
- <sup>16</sup>S. Rubini and P. Ballone, *Phys. Rev. B* **48**, 99 (1993).
- <sup>17</sup>G. P. Srivastava, *The Physics of Phonons* (Hilger, Bristol, 1990).
- <sup>18</sup>A. A. Maradudin, P. A. Flinn, and R. A. Coldwell-Horsfall, *Ann. Phys. (N.Y.)* **15**, 337 (1961); A. A. Maradudin and P. A. Flinn, *Phys. Rev.* **129**, 2529 (1963).
- <sup>19</sup>G. Leibfried and W. Ludwig, *Theory of Anharmonic Effects in Crystals* (Academic, New York, 1961).
- <sup>20</sup>J. Rosen and G. Grimvall, *Phys. Rev. B* **27**, 7199 (1983).
- <sup>21</sup>Van de Walle, G. Ceder, and U. V. Waghmare, *Phys. Rev. Lett.* **80**, 4911 (1998).
- <sup>22</sup>Van de Walle and G. Ceder, *Phys. Rev. B* **61**, 5972 (2000).
- <sup>23</sup>T. Yokoyama, Y. Yonamoto, T. Ohta, and A. Ugawa, *Phys. Rev. B* **54**, 6921 (1996).
- <sup>24</sup>T. Yokoyama, K. Kobayashi, T. Ohta, and A. Ugawa, *Phys. Rev. B* **53**, 6111 (1996).
- <sup>25</sup>A. I. Frenkel and J. J. Rehr, *Phys. Rev. B* **48**, 585 (1993).
- <sup>26</sup>N. Boccara and G. Sarma, *Physics (N.Y.)* **1**, 219 (1965).
- <sup>27</sup>N. S. Gillis, N. R. Werthamer, and T. R. Koehler, *Phys. Rev. B* **165**, 951 (1968).
- <sup>28</sup>P. F. Choquard, *The Anharmonic Crystal* (Benjamin, New York 1967).
- <sup>29</sup>R. C. Shukla and E. Sternin, *Philos. Mag. B* **74**, 1 (1996).
- <sup>30</sup>R. Hardy, M. A. Day, R. C. Shukla, and E. R. Cowley, *Phys. Rev. B* **49**, 8732 (1994).
- <sup>31</sup>R. C. Shukla, *Philos. Mag. B* **74**, 13 (1996), *Phys. Status Solidi B* **205**, 481 (1998).
- <sup>32</sup>F. Ducastelle, *J. Phys. (France)* **31**, 1055 (1970).
- <sup>33</sup>R. P. Gupta, *Phys. Rev. B* **23**, 6265 (1981); D. Tomanenk, S. Mukherjee, and K. H. Bennemann, *ibid.* **28**, 665 (1983); W. Zhong, Y. S. Li, and D. Tomanek, *ibid.* **44**, 13053 (1991).
- <sup>34</sup>M. W. Finnis and J. E. Sinclair, *Philos. Mag. A* **50**, 45 (1984).
- <sup>35</sup>V. Rosato, M. Guillope, and B. Legrand, *Philos. Mag. A* **59**, 321 (1989).
- <sup>36</sup>F. Cleri and V. Rosato, *Phys. Rev. B* **48**, 22 (1993).
- <sup>37</sup>B. von Sydow, J. Hartford, and G. Wahnstrom, *Comput. Mater. Sci.* **15**, 367 (1999).
- <sup>38</sup>C.-H. Chien, E. Blaisten-Barojas, and M. R. Pederson, *J. Chem. Phys.* **112**(5), 2301 (2000).
- <sup>39</sup>M. M. Sigalas and D. A. Papaconstantopoulos, *Phys. Rev. B* **49**, 1574 (1994).

- <sup>40</sup>Y. Li, E. B. Barojas, and D. A. Papaconstantopoulos, *Phys. Rev. B* **57**, 15519 (1998).
- <sup>41</sup>M. S. Daw and M. I. Baskes, *Phys. Rev. B* **29**, 6443 (1984).
- <sup>42</sup>S. M. Foiles, M. I. Baskes, and M. S. Daw, *Phys. Rev. B* **33**, 7983 (1986).
- <sup>43</sup>M. I. Baskes, *Phys. Rev. Lett.* **59**, 2666 (1987).
- <sup>44</sup>J. M. Holender, *Phys. Rev. B* **41**, 8054 (1990).
- <sup>45</sup>R. Pasionot, D. Farkas, and E. J. Savino, *Phys. Rev. B* **43**, 6952 (1991).
- <sup>46</sup>L. A. Girifalco and V. G. Weizer, *Phys. Rev.* **114**, 687 (1959).
- <sup>47</sup>N. V. Hung and J. J. Rehr, *Phys. Rev. B* **56**, 43 (1997).
- <sup>48</sup>U. Hansen, P. Vogl, and V. Fiorentini, *Phys. Rev. B* **60**, 5055 (1999).
- <sup>49</sup>N. Tang and V. V. Hung, *Phys. Status Solidi B* **149**, 511 (1988); V. E. Panhim *et al.*, *Phase Theory in Alloys* (Nauka, Novosibirsk, 1984) (in Russian).
- <sup>50</sup>N. Tang and V. V. Hung, *Phys. Status Solidi B* **162**, 371 (1990).
- <sup>51</sup>Vu Van Hung and K. Masuda-Jindo, *J. Phys. Soc. Jpn.* **69**, 2067 (2000); V. V. Hung, H. V. Tich, and K. Masuda-Jindo, *ibid.* **69**, 2691 (2000).
- <sup>52</sup>D. Frenkel and A. J. C. Ladd, *J. Chem. Phys.* **81**, 3188 (1984).
- <sup>53</sup>D. Frenkel, *Phys. Rev. Lett.* **56**, 858 (1986).
- <sup>54</sup>Ya. P. Terletsy and N. Tang, *Ann. Phys. (Leipzig)* **19**, 299 (1967).
- <sup>55</sup>S. S. Mitra and S. K. Joshi, *J. Chem. Phys.* **34**, 1462 (1961).
- <sup>56</sup>K. A. Gschneidner Jr., *Solid State Phys.* **16**, 275 (1964).
- <sup>57</sup>*American Institute of Physics Handbook*, 3rd ed., edited by B. H. Billings *et al.* (McGraw-Hill, New York, 1982).
- <sup>58</sup>M. W. Zemansky, *Heat and Thermodynamics* (McGraw-Hill, New York, 1957), p. 263.
- <sup>59</sup>J. Mei, J. W. Davenport, and G. W. Fernando, *Phys. Rev. B* **43**, 4653 (1991).
- <sup>60</sup>N. I. Papanicolaou, G. C. Kallinteris, G. A. Evangelakis, and D. A. Papaconstantopoulos, *Comput. Mater. Sci.* **17**, 224 (2000).
- <sup>61</sup>R. C. Shukla and C. A. Plint, *Phys. Rev. B* **40**, 10 337 (1989), and references therein.
- <sup>62</sup>M. Simerska, *Acta Crystallogr.* **14**, 1259 (1961); *Czech. J. Phys.* **B12**, 858 (1962).
- <sup>63</sup>R. Kikuchi, *Phys. Rev.* **81**, 998 (1951); T. Mohri, J. M. Sanchez, and D. de Fontaine, *Acta Metall.* **33**, 1171 (1985).
- <sup>64</sup>R. Kikuchi and K. Masuda-Jindo, *Comput. Mater. Sci.* **8**, 1 (1997).
- <sup>65</sup>A. Finel, *Suppl. Prog. Theor. Phys.* **115**, 59 (1994); A. Finel and R. Tétot, in *Stability of Materials*, edited by A. Gonis, P.E.A. Turchi, and J. Kudrnovsky, NATO ASI Series, Vol. 355 (Plenum, New York, 1996), p. 197.
- <sup>66</sup>R. A. MacDonald, R. C. Shukla, and D. K. Kahalner, *Phys. Rev. B* **29**, 6489 (1984).
- <sup>67</sup>D. Porezag, Th. Kohler, G. Seifert, and R. Kaschner, *Phys. Rev. B* **51**, 12947 (1995); Th. Frauenheim, F. Weich, Th. Kohler, S. Uhlmann, D. Porezag, and G. Seifert, *Phys. Rev. B* **52**, 11492 (1995).
- <sup>68</sup>R. E. Cohen, M. J. Mehl, and D. A. Papaconstantopoulos, *Phys. Rev. B* **50**, 14 694 (1994); E. Wasserman, L. Stixrude, and R. E. Cohen, *ibid.* **53**, 8296 (1996).
- <sup>69</sup>P. Giannozzi, S. de Gironcoli, P. Pavone, and S. Baroni, *Phys. Rev. B* **43**, 7231 (1991).
- <sup>70</sup>D. J. Kouri, Y. Huang, and D. K. Hoffman, *J. Phys. Chem.* **100**, 7903 (1996); J. M. Thijssen and J. E. Inglesfield, *Phys. Rev. B* **51**, 17 988 (1995).